Published in final edited form as:
Mol Pharmacol. 2012 May ; 81(5): 719–728. doi:10.1124/mol.111.077321.

Anticancer Activity of Methyl-Substituted Oxaliplatin Analogs†

Ute Jungwirth, **Dimitris N. Xanthos**, **Johannes Gojo**, **Anna K. Bytzek**, **Wilfried Körner**, **Petra Heffeter**, **Sergey A. Abramkin**, **Michael A. Jakupec**, **Christian G. Hartinger**, **Ursula Windberger**, **Markus Galanski**, **Bernhard K. Keppler**, and **Walter Berger**
Institute of Cancer Research, Department of Medicine I, Medical University of Vienna, Vienna, Austria (U.J., J.G., P.H., W.B.); Comprehensive Cancer Centre of the Medical University of Vienna, Vienna, Austria (U.J., J.G., P.H., W.B.); Research Platform "Translational Cancer Therapy Research Vienna," Vienna, Austria (U.J., J.G., P.H., M.A.J., C.G.H., M.G., B.K.K., W.B.); Department of Neurophysiology, Centre for Brain Research, Medical University of Vienna, Vienna, Austria (D.N.X.); Institute of Inorganic Chemistry, University of Vienna, Vienna, Austria (A.K.B., S.A.A., M.A.J., C.G.H., M.G., B.K.K.); Department of Environmental Geosciences, University of Vienna, Vienna, Austria (W.K.); and Division for Biomedical Research, Medical University of Vienna, Vienna, Austria (U.W.)

Abstract

Oxaliplatin is successfully used in systemic cancer therapy. However, resistance development and severe adverse effects are limiting factors for curative cancer treatment with oxaliplatin. The purpose of this study was to comparatively investigate in vitro and in vivo anticancer properties as well as the adverse effects of two methyl-substituted enantiomerically pure oxaliplatin analogs [[(1*R*,2*R*,4*R*)-4-methyl-1,2-cyclohexanediamine] oxalatoplatinum(II) (KP1537), and [(1*R*,2*R*,4*S*)-4-methyl-1,2-cyclohexanediamine]oxalatoplatinum(II) (KP1691)] and to evaluate the impact of stereoisomerism. Although the novel oxaliplatin analogs demonstrated in multiple aspects activities comparable with those of the parental compound, several key differences were discovered. The analogs were characterized by reduced vulnerability to resistance mechanisms such as p53 mutations, reduced dependence on immunogenic cell death induction, and distinctly attenuated adverse effects including weight loss and cold hyperalgesia. Stereoisomerism of the substituted methyl group had a complex and in some aspects even contradictory impact on drug accumulation and anticancer activity both in vitro and in vivo. To summarize, methyl-substituted oxaliplatin analogs harbor improved therapeutic characteristics including significantly reduced adverse effects. Hence, they might be promising metal-based anticancer drug candidates for further (pre)clinical evaluation.

†The online version of this article (available at http://molpharm.aspetjournals.org) contains supplemental material.

Address correspondence to: Dr. Walter Berger, Institute of Cancer Research, Medical University of Vienna, Borschkegasse 8a, 1090 Vienna, Austria. walter.berger@meduniwien.ac.at.

Authorship Contributions

Participated in research design: Jungwirth, Xanthos, Heffeter, Hartinger, and Berger.
Conducted experiments: Jungwirth, Xanthos, Gojo, and Bytzek.
Contributed new reagents or analytic tools: Xanthos, Bytzek, Körner, Abramkin, Jakupec, Windberger, Galanski, Keppler, and Berger.
Performed data analysis: Jungwirth, Xanthos, Gojo, Bytzek, Körner, Heffeter, and Hartinger.
Wrote or contributed to the writing of the manuscript: Jungwirth, Hartinger, Galanski, and Berger.

This work was previously presented in part in the following publications: Jungwirth U, Heffeter P, Gojo J, Abramkin S, Meelich K, Körner W, Micksche M, Galanski M, Keppler BK, and Berger W (2010) Stereoisomerism significantly impacts on the anticancer activity of novel oxaliplatin analogues in vitro and in vivo (Poster 447). *Eur J Cancer Suppl* **8 (7):**141; Jungwirth U, Heffeter P, Gojo J, Abramkin S, Meelich K, Galanski M, Körner W, Micksche MM, and Berger W (2009) Novel monosubstituted oxaliplatin analogs with improved characteristics. *Mol Cancer Ther* **8 (12 Suppl):**C93; and Jungwirth U, Heffeter P, Jakupec MA, Micksche MM, Keppler BK, and Berger W (2007) Anticancer activities of new oxaliplatin derivatives (Abstract P043). *J Biol Inorg Chem* **12 (Suppl 1):**S35.

Europe PMC Funders Author Manuscripts

Introduction

Metal-based drugs have been key players in systemic anticancer therapy since the discovery of the anticancer activity of *cis*-diamminedichloridoplatinum(II) (cisplatin) in the 1960s (Rosenberg et al., 1965, 1969). However, unwanted side effects and especially the resistance of tumor cells limit curative clinical applications of cisplatin. Whereas a large subset of tumors exhibits intrinsic resistance, those cancer types initially responsive to platinum drugs often develop cisplatin-resistant recurrences or metastasis (Heffeter et al., 2008). Although numerous additional metal compounds have been synthesized, only a few have been successful in clinical trials. In the case of platinum-based anticancer drugs, only cisplatin, [(1*R*,2*R*)-cyclohexanediamine] (oxaliplatin), and *cis*-diammine(1,1-cyclobudandicarboxylato)platinum(II) (carboplatin) are used in clinical routines (Shah and Dizon, 2009).

The third-generation platinum drug oxaliplatin was approved in 2004 as a standard treatment of advanced metastatic colorectal carcinoma in combination with 5-fluorouracil and leucovorin (FOLFOX) (Goldberg et al., 2004). With regard to adverse effects, cisplatin causes both nephrotoxicity and neurotoxicity, whereas oxaliplatin primarily induces the latter. Even though oxaliplatin-induced neurotoxicity is more rapidly reversible than the neurotoxicity caused by cisplatin, it remains the dose-limiting factor (Stordal et al., 2007). Severe acute and/or chronic neurotoxic effects are observed in the majority of patients, frequently requiring dose reduction or treatment termination even without tumor progression (McWhinney et al., 2009). Different strategies to prevent and/or manage oxaliplatin-induced neurotoxicity, including prophylactic and systematic treatments, have been introduced. However, randomized trials demonstrating effectiveness are still missing (Ali, 2010). In a recent study, it has been shown that organic cation/carnitine transporter-mediated uptake of oxaliplatin might contribute to its neuronal accumulation and treatment-limiting neurotoxicity (Jong et al., 2011).

In general, intracellular oxaliplatin uptake is still not fully understood, and both passive diffusion (Luo et al., 1999) and lipophilicity-independent transporter-mediated uptake are discussed (Burger et al., 2010; Buss et al., 2011). Inside the cell, platinum drugs are believed to predominantly target DNA. Of interest, cisplatin and oxaliplatin form similar DNA adducts, but the total amount of platination is substantially lower for oxaliplatin (Woynarowski et al., 1998). Furthermore, the hydrophobic and bulkier ligand of oxaliplatin is recognized differently by mismatch repair proteins, DNA polymerases, and damage recognition proteins (Chaney et al., 2005). The disturbance of the DNA structure ultimately leads to cell cycle arrest and apoptosis (Wang and Lippard, 2005). However, because only traces of intravenously administered platinum drugs reach tumor cell DNA, some recent studies suggested the existence of extranuclear targets underlying both cisplatin- and oxaliplatin-induced cytotoxicity (Kelland, 2007; Heffeter et al., 2008; Pizarro and Sadler, 2009; Jungwirth et al., 2011). On the basis of the knowledge that the cyclohexanediamine (DACH) ligand) with *trans-R,R* configuration is a determining factor of the specific oxaliplatin activity (Pendyala et al., 1995), enantiomerically pure oxaliplatin derivatives with an equatorial methyl group at position 4 of the cyclohexane ring have been synthesized (Galanski et al., 2004; Habala et al., 2005; Abramkin et al., 2010). A pilot feasibility study revealed that these novel oxaliplatin derivatives exhibit promising activity against a mouse leukemia model in vivo (Abramkin et al., 2010). In the present study we comprehensively analyzed the in vitro and in vivo activity of the two stereoisomeric lead compounds, namely [(1*R*,2*R*,4*R*)-4-methyl-1,2-cyclohexanediamine]oxalatoplatinum (II) (KP1537) and [(1*R*,2*R*,4*S*)-4-methyl-1,2-cyclohexanediamine]oxalatoplatinum(II) (KP1691) (Fig. 1, A–C). Of interest, the presence and stereoisomerism of even one methyl group substituted at the

cyclohexane ring had a major and complex influence on anticancer activities in vitro and in vivo.

Materials and Methods

Reagents

Oxaliplatin, KP1537, and KP1691 were prepared at the Institute of Inorganic Chemistry, University of Vienna (Vienna, Austria). Synthesis and characterization have been reported recently (Abramkin et al., 2010). The oxalatoplatinum(II) complexes were fully characterized by elemental analysis and multinuclear (^{1}H, ^{13}C, and ^{195}Pt) one- and two-dimensional NMR spectroscopy. The enantiomeric and diastereomeric purity was proven by chiral high-performance liquid chromatography. For in vitro studies, compounds were dissolved in water and diluted in culture media at the indicated concentrations. For in vivo studies, oxaliplatin and analogs were dissolved in 5% glucose. Cisplatin was dissolved in dimethylformamide and diluted in culture media. All other substances were purchased from Sigma-Aldrich (St. Louis, MO). All solutions were freshly prepared before use.

Cell Culture

The cancer cell lines and media used in this study are given in Supplemental Fig. 1. All culture media were supplemented with 10% fetal calf serum (PAA, Linz, Austria). All cells were cultured at 37°C in a humidified atmosphere and 5% CO_2. Cultures were periodically checked for *Mycoplasma* contamination. The cell lines were authenticated in all cases by (array) comparative genomic hybridization when this study was started (44K human whole-genome DNA arrays; Agilent Technologies, Santa Clara, CA).

Cytotoxicity Assay

Cancer cells (2×10^3) were exposed to oxaliplatin, KP1537, and KP1691 for the indicated time and concentration. Anticancer activity was determined by reduction of mitochondrial activity with a 3-(4,5-dimethylthiazol-2-yl)-2,5-diphenyltetrazolium bromide (MTT)-based vitality assay (EZ4U; Biomedica, Vienna, Austria) (Heffeter et al., 2007). Cytotoxicity was expressed as IC_{50} values calculated from full dose-response curves. Experiments were performed in triplicate and repeated three times. Resistance factors were calculated by dividing the IC_{50} of the parental cell line by the IC_{50} of the sub-/resistant cell line.

Annexin V/PI Staining

HCT-116 cells (3×10^5) were exposed to the platinum drugs for 24 or 48 h. Cells were stained with annexin V (annexin V-FITC; BD Biosciences, San Jose, CA) and propidium iodide (200 ng/ml PI; Sigma-Aldrich) and analyzed according to the manufacturer's protocol by flow cytometry using fluorescence-activated cell sorting (FACSCalibur; BD Biosciences). CellQuest Pro software (BD Biosciences) was used to analyze the data. Experiments were repeated three times.

Western Blot Analysis

HCT-116 cells (3×10^5) were exposed to 10 μM oxaliplatin, KP1691, and KP1537 for 24 or 48 h. Total protein lysates were prepared, resolved by SDS-polyacrylamide gel electrophoresis, and transferred onto a polyvinylidene difluoride membrane for Western blotting according to Berger et al. (1994) and Heffeter et al. (2007). Nuclear proteins were extracted with the NE-PER Nuclear and Cytoplasmic Extraction kit (Thermo Fisher Scientific, Waltham, MA). The antibody against p53 was from Thermo Fisher Scientific. A complete list of primary antibodies is given in Supplemental Fig. 2. Secondary horseradish peroxidase-labeled antibodies from Santa Cruz Biotechnology, Inc. (Santa Cruz, CA) were

Europe PMC Funders Author Manuscripts

used at working dilutions of 1:10,000. Western blot bands were quantified with QuantiScan software (Biosoft, Cambridge, UK).

Platinum Accumulation and Distribution

HCT-116 cells (3×10^5) were exposed to 10 μM oxaliplatin, KP1691, or KP1537 at 37°C. Total, cytosolic, and particulate accumulated platinum was determined according to methods published previously (Heffeter et al., 2010). For DNA platination (10^6 cells), DNA was isolated with a phenol-chloroform extraction, and DNA amounts were quantified with a NanoDrop spectrophotometer. All samples were lysed in tetramethylammonium hydroxide and diluted in 0.6 N HNO_3, and platinum concentrations were determined by inductively coupled plasma mass spectrometry using an Elan 6100 (PerkinElmerSciex Instruments, Boston, MA) (Heffeter et al., 2010). Results are expressed as platinum amount per cell, milligrams of protein, or milligrams of DNA. Values represent the means of at least three independent experiments.

In Vivo Experiments

Six- to 8-week-old female SCID/BALB/c, BALB/c, and DBA/2J mice were purchased from Harlan (San Pietro al Natisone, Italy). For xenograft experiments, animals were kept in a pathogen-free environment, and every procedure with the SCID/BALB/c mice was done in a laminar airflow cabinet. Animals for behavioral experiments were kept in conventional cages. The experiments were done according to the Federation of Laboratory Animal Science Association guidelines for the use of experimental animals and were approved by the Ethics Committee for the Care and Use of Laboratory Animals at the Medical University Vienna and the Ministry of Science and Research, Austria.

Solid Tumor Xenograft Model

For local tumor growth experiments, 5×10^5 CT-26 cells were injected subcutaneously into the right flank of SCID/BALB/c and BALB/c mice (day 0). Animals were randomly assigned to treatment groups, and therapy was started when tumors were palpable. Animals were treated with oxaliplatin, KP1537, or KP1691 intravenously (9 mg/kg dissolved in 5% glucose for 2 weeks, twice per week). Animals in the control group received 100 μl of a 5% glucose solution. Animals were controlled for distress development every day, and tumor size was assessed regularly by caliper measurement. Tumor volume was calculated using the formula [(length × width^2) × 0.5] (Fischer et al., 2008). Mouse body weight was determined at baseline before drug administration and was recorded regularly during the experiment.

In Vivo Platinum Accumulation

CT-26 cells (5×10^5) were injected subcutaneously into the right flank of BALB/c mice (day 0). Animals were randomly assigned to treatment groups and treated with one intravenous injection of oxaliplatin, KP1537, or KP1691 (9 mg/kg dissolved in 5% glucose). Animals were sacrificed after 1 or 6 h. Tumor and organ samples were digested with 34% nitric acid in a microwave system (MLS-Ethos1600; Milestone-MLS GmbH, Leutkirchen, Germany). The platinum content was determined by inductively coupled plasma mass spectrometry (Agilent 7500ce; Agilent Technologies, Waldbronn, Germany) (Heffeter et al., 2010).

Behavioral Testing

BALB/c mice were habituated to the animal facility for at least 2 weeks. They were then handled by the experimenter and habituated to the various behavioral testing apparatus. Mice were randomized to treatment groups ($n = 8$) of either 5% glucose solution, oxaliplatin (9 mg/kg), or KP1537 (9 mg/kg). As in the xenograft experiments, mice were treated

Europe PMC Funders Author Manuscripts

intravenously for 2 weeks, twice per week (weeks 1 and 2). Mouse body weight was determined at baseline before drug administration and was recorded during the experiment. Experiments were performed in a blinded fashion with the experimenter unaware of the treatment group.

Activity Monitoring

Locomotor activity was monitored at baseline (1 week before treatment) and similar to in vivo anticancer activity during drug treatment at weeks 1 and 2 and after treatment in week 3. Mice were placed in the middle of the open chamber box (40 × 60 cm, low lightning condition) and allowed to run freely for 1 min before behavioral recording for 3 min, similar to previously described measurements of the locomotor activity in mice after oxaliplatin or cisplatin treatment (Ta et al., 2009). The measurement was repeated three times per test day. Distances covered were video-recorded and measured.

Cold Plate Assay

To test for cold hyperalgesia, animals are placed on a −4°C hot-cold plate (Bioseb, Vitrolles, France). In preliminary experiments (data not shown), this was found to be an optimal temperature to induce significant nociceptive behaviors to detect cold hyperalgesia as shown previously (Ta et al., 2009). The total number of paw lifting/licking behaviors within a 1-min period was measured. Movements associated with locomotion were excluded. Mice were only tested once on any given test day to avoid any sensitization or stress effects.

Heat Assay

To test for heat hyperalgesia, animals were placed on a +54°C hot-cold plate (Bioseb). The latency time to the first nociceptive behavior (paw stamping or licking) was measured (Ta et al., 2009). Movements associated with locomotion were excluded. The measurement was repeated three times per test day.

Statistics

All data are expressed as mean ± S.D. Results were analyzed and illustrated with GraphPad Prism (version 5; GraphPad Software, San Diego, CA). Statistical analyses were performed using two-way ANOVA with drug treatment, time, or cell type as independent variables and conducted with Bonferroni post-tests to examine the differences between the different drug treatment regimens and the diverse responses. A p value of 0.05 was considered statistically significant.

Results

Effects of Novel Oxaliplatin Derivatives on Viability and Proliferation of Human Tumor Cell Models

The anticancer activities of KP1537 (with an equatorial methyl group) and KP1691 (with an axial methyl group) were compared with those of oxaliplatin (Fig. 1) in several cell models derived from human and murine solid tumors (cervix, lung, breast, and colon) as well as leukemia. Cell viability was determined by MTT assay after 72 h of drug treatment (Table 1). In general, all three substances had IC_{50} values in the low micromolar range. The significantly lower IC_{50} values of KP1691 were remarkable compared with those for oxaliplatin and its stereoisomer KP1537 in almost all cell models. The mean IC_{50} value for all investigated cell lines of oxaliplatin was 1.9 μM and 1.0 and 2.2 μM for KP1691 and KP1537, respectively (calculated from Table 1). In addition, clonogenic assays were performed to prove the growth inhibition of oxaliplatin, KP1537, and KP1691. The outcome confirmed the MTT assay results (data not shown).

Because of the known impact of p53 on the activity of oxaliplatin, we analyzed isogenic cell models with different specific gene disruptions. When HCT-116 parental cells (p53/wt, p21/wt, and bax/wt) were compared with their sublines (p53/ko, p21/ko, and bax/ko) the expected influence of p53 on oxaliplatin and its analogs was observed (Table 1). IC_{50} values of the p53/ko subline were approximately 3.1-fold higher for oxaliplatin, 2.3-fold higher for KP1537, and 1.7-fold higher for KP1691 compared with values for the parental cell line. This result indicates that the activity of the novel oxaliplatin analogs is less susceptible to the p53 mutation status compared with that for oxaliplatin.

In pulsing experiments (72-h survival with short-time drug exposure), at 2 h of treatment KP1691 produced greater cytotoxicity than oxaliplatin and KP1537 in both the p53/wt (Supplemental Fig. 3) and p53/ko background (data not shown). The impact of p21 and bax was less pronounced than that of p53, and all resistance factors were less than 1.7. In addition, in the p21/ko and bax/ko cell models, KP1691 exerted the highest cytotoxicity. In a previous study (Abramkin et al., 2010), we showed that, as for oxaliplatin, KP1537 and KP1691 are also moderately but significantly cross-resistant to cisplatin-resistant cell models. To test the impact of oxaliplatin resistance, we selected HCT-116 p53/wt and p53/ko cells against oxaliplatin, generating the cell models HCT-116 p53/wt oxR (Abramkin et al., 2010) and HCT-116 p53/ko oxR (Fig. 1, D and E). Cross-resistance of KP1537 and KP1691 was highly significant (Fig. 1, F and G), but in all cases the resistance factors (Fig. 1H) were lower than those for oxaliplatin.

Differences in Cellular Platinum Accumulation, Distribution, and DNA Binding

To determine whether the differences in sensitivity to the tested oxaliplatin analogs were accompanied by altered platinum accumulation, HCT-116 p53/wt cells were exposed to 10 μM oxaliplatin, KP1537, or KP1691 for 4 and 24 h. Of interest, there was a significantly higher accumulation of (the less cytotoxic) KP1537 compared with equimolar oxaliplatin or KP1691 at both time points. At 4 h, KP1537 accumulation was already 2.1- and 1.6-fold higher than oxaliplatin or KP1691 levels, respectively. After 24 h, the respective values ranged to 1.9- and 1.6-fold (Fig. 2A, left). Similar data were obtained with HCT-116 p53/ko cells (Supplemental Fig. 4A). However, washout experiments suggested a distinctly different interaction of the compounds with cellular targets. Although almost no cell-associated platinum was lost during the 4-h drug-free postincubation with oxaliplatin and KP1691, almost half of KP1537 was lost (Fig. 2A, right). Nevertheless, the cellular platinum content still remained significantly higher with KP1537 than with oxaliplatin but not KP1691. Next, we analyzed the distribution of the different platinum compounds between the cytosolic and the nucleic/particulate fractions (Fig. 2B). For all three compounds, approximately 80% of platinum was found in the cytosol and 20% in the nucleic/particulate fractions of HCT-116 p53/wt cell. Thus, also in the nucleic/particulate fraction, platinum levels were highest for KP1537. A similar pattern could be detected in HCT-116 p53/ko cells, with slightly higher platinum levels in the nucleic/particulate fraction (Supplemental Fig. 4B). Furthermore, independent of p53 status, the two novel substances led to significantly higher amounts of platinum bound to DNA (2-fold) than to oxaliplatin (Fig. 2C). Taken together, the significantly higher binding of both novel compounds to DNA but the general higher washout of KP1537 may explain the different effects of the stereoisomers on cell activity in vitro.

Impact of KP1537 and KP1691 on Cell Cycle Distribution

The impact of the oxaliplatin analogs on cell cycle progression was determined in HCT-116 p53/wt and p53/ko cells by fluorescence-activated cell sorting analysis after 24 h (Supplemental Fig. 5) and 48 h (Supplemental Fig. 6) of drug exposure. In general, no significant differences were observed regarding the impact of the three platinum compounds

on the cell cycle distribution and cell cycle-related protein expression pattern. To determine the effects of the novel oxaliplatin drugs on DNA synthesis in HCT-116 p53/wt and p53/ko cells, [^{3}H]thymidine incorporation assays were performed (Supplemental Fig. 7). Almost complete inhibition of DNA synthesis was already observed at 2.5 μM after 24 h with all three drugs in HCT-116 p53/wt cells. Comparable to the MTT data, a significant difference between HCT-116 p53/wt and p53/ko cells was detected.

Induction of Apoptosis

Besides cell cycle inhibition, oxaliplatin exerts its activity via induction of apoptosis. Annexin V/PI staining revealed that KP1537, although less active in MTT assays, induced a significantly higher amount of early apoptosis (annexin V^+/PI^-) than oxaliplatin and KP1691 in HCT-116 p53/wt cells after 24 h of exposure (Fig. 3, A and B). Furthermore, KP1537 induced the highest levels of late apoptosis (annexin V^+/PI^+) after 48 h, followed by KP1691 (Fig. 3, C and D). As expected, induction of apoptosis was stronger in HCT-116 p53/wt (Fig. 3, A and C) than in p53/ko cells (Fig. 3, B and D) with all tested drugs. The higher levels of KP1537-induced apoptosis could be confirmed by staining with JC-1, a marker for the loss of mitochondrial membrane potential as an early event in apoptosis by the intrinsic pathway (Supplemental Fig. 8). Accordingly, poly-(ADP-ribose) polymerase cleavage was highest for KP1537 in HCT-116 p53/wt and p53/ko cells (Fig. 3, E and F), and after 24 h enhanced phosphorylation of p53 and H2AX in the nucleus could be detected (Fig. 3G).

In Vivo Anticancer Activity

In vivo anticancer activity of the platinum compounds investigated was analyzed in a colon cancer xenograft model (Fig. 4A and B). In a previous study, we demonstrated an enhanced therapeutic window and consequently enhanced activity for KP1537 compared with those for oxaliplatin and KP1691 against the murine leukemic L1210 model (Abramkin et al., 2010).

When the murine leukemic model was compared with a solid colon carcinoma model (CT-26), a completely different picture emerged. Because of the recently reported importance of the immune system driving the anticancer activity of oxaliplatin (Tesniere et al., 2010), we decided to compare immunocompetent BALB/c (Fig. 4A) with immunodeficient SCID/BALB/c (Fig. 4B) mice. Therefore, CT-26-bearing mice were treated intravenously twice a week for 2 weeks with 5% glucose solution or 9 mg/kg oxaliplatin, KP1537, or KP1691 as soon as the tumor was palpable. Almost no anticancer activity was detected for oxaliplatin in the immunodeficient SCID/BALB/c mice. This inefficacy is in accordance with previously published data describing the necessity of an active immune response for the anticancer activity of oxaliplatin (Tesniere et al., 2010). It is of note that solid colon cancer xenograft growth was significantly retarded by both novel platinum drugs compared with that in control and oxaliplatin-treated mice in the immunodeficient SCID/BALB/c mice (Fig. 4A). In contrast to the leukemic xenograft model, the difference between the two oxaliplatin analogs was minor. Whereas tumor growth retardation became significant on day 9 after first treatment with KP1537, this occurred at day 12 with KP1691. Growth retardation remained significant for both novel complexes until termination of the experiment. Oxaliplatin retarded tumor growth very transiently, resulting only on day 15 in a significant (**, $p < 0.01$) inhibition compared with that in control mice, whereas data for all other days were not significant (Fig. 4A). In immunocompetent BALB/c mice, all three platinum drugs, including oxaliplatin, were active and retarded significantly (***, $p < 0.001$) the growth of the CT-26 tumors from day 18 until experiment termination (Fig. 4B).

Europe PMC Funders Author Manuscripts

Adverse Effects

Maximal tolerated dose analysis suggested lower systemic toxicity of the novel analogs compared with that of oxaliplatin. In addition, in the CT-26 xenograft experiments, mice treated with KP1537 or KP1691 were in better health than the oxaliplatin group. Whereas oxaliplatin-treated mice frequently remained in a hunched posture, KP1537- and KP1691-treated mice were more active and comparable to control animals. Because CT-26 tumors induce cachexia in mice, it was impossible to determine the drug-induced weight changes. Therefore, the weight loss and development of side effects was monitored in tumor-free BALB/c mice. Because KP1537 was as active as oxaliplatin in the BALB/c model at equimolar concentrations and more active compared with oxaliplatin and KP1691 in vivo, at least in the leukemic model, we decided to designate KP1537 as the lead compound. Thus, KP1537 has been compared with oxaliplatin in all adverse effect studies. Mice treated with the platinum compounds lost weight (Fig. 5A), whereby the effect was significantly stronger with oxaliplatin. Remarkably, KP1537-treated mice recovered more rapidly, and body weight was already comparable with that of control mice 2 weeks after therapy. In contrast, oxaliplatin-treated mice still exhibited significantly (***, $p < 0.001$, two-way ANOVA) reduced body weight at that time point.

Treatment with oxaliplatin also resulted in significantly reduced levels of locomotor activity. Whereas vehicle- and KP1537-treated mice became significantly more active and explorative during the experiment, the activity of oxaliplatin-treated mice remained almost at baseline levels (Fig. 5B).

Cold hypersensitivity is one of the major adverse symptoms of oxaliplatin-induced neuropathy in the clinical routine (Ali, 2010). Therefore, we tested whether mice treated with oxaliplatin or KP1537 were hypersensitive to cold or heat (Fig. 5, C and D). At baseline, there was no significant difference between the groups, neither with a cold nor a hot stimulus ($p > 0.05$, two-way ANOVA). In accordance with other studies (Ta et al., 2009), thermal hyperalgesia was not detected as a consequence of oxaliplatin or the novel platinum compound (Fig. 5C). In contrast, already during the first therapy week, a moderately, nonsignificantly increased hypersensitivity toward cold was detected in oxaliplatin- and KP1537-treated mice. After the second treatment cycle, only oxaliplatin-treated mice had a significant (3-fold) increase in the number of paw lifts after cold stimuli compared with those for glucose-treated controls (5.7 versus 18.1, *, $p < 0.05$). This cold hyperalgesia persisted and was even stronger 1 week after oxaliplatin therapy was stopped in week 3 (6-fold, 4.6 versus 28.3, ***, $p < 0.01$). Even though there was a tendency toward an increase of paw lifts after KP1537 treatment, no significant hyperalgesia was observed throughout the experiment. These data are corroborated by platinum accumulation studies of the sciatic nerve. Mice treated with a bolus injection of oxaliplatin or KP1537 (9 mg/kg) showed different platinum accumulation levels (Fig. 5E). Similar to that in the tumor samples, platinum accumulation in oxaliplatin-treated animals increased significantly from 1 to 6 h, whereas this effect was not observed after KP1537 therapy. Two-fold enhanced platinum was detected in the sciatic nerve after oxaliplatin compared with KP1537 administration. In contrast, no significant difference could be detected in platinum levels of other organs such as liver (Fig. 5F), spleen (Fig. 5G), and kidney (Fig. 5H), even though there was a tendency for higher platinum content in oxaliplatin-treated animals. Of interest, the in vivo anticancer activity did not correlate with the in vivo platinum accumulation in the CT-26 tumors. After 1 h, oxaliplatin and KP1537 accumulated approximately to the same levels in the tumor tissue (Fig. 5I). Over time there was no change in KP1537 accumulation, whereas oxaliplatin significantly increased (**, $p < 0.1$, two-way ANOVA). Even though there was less KP1537 found in the tumor tissue, the novel drug was as active as oxaliplatin against CT-26 tumors in the SCID background and demonstrated significantly higher activity in the BALB/c background (compare Fig. 4, A and B).

Discussion

During the past few years, several approaches have been taken to improve anticancer activity and pharmacologic properties of oxaliplatin including encapsulation (Abu Lila et al., 2010), modifications at its leaving group, and/or synthesis of analogous platinum(IV) complexes (Reithofer et al., 2007; Wang, 2010). Oxaliplatin analogs with substituents at the cyclohexane ligand were so far solely reported by our group, and initial data have suggested that these compounds might be of interest for further (pre)clinical development (Galanski et al., 2004; Habala et al., 2005; Abramkin et al., 2010). Here, we present preclinical in vitro and in vivo data regarding the anticancer activity of two lead stereoisomeric oxaliplatin analogs, namely KP1537 and KP1691, derivatized at position 4 of the cyclohexane ring with an equatorial or axial methyl group, respectively (Galanski et al., 2004; Habala et al., 2005; Abramkin et al., 2010). Taken together, our results suggest 1) superiority of the derivatives compared with oxaliplatin on the basis of improved therapeutic windows and 2) an unexpectedly complex impact of the minor derivatization and the related stereoisomerism on cancer (cell) accumulation and anticancer activity both in vitro and in vivo.

Besides adverse effects, intrinsic and/or acquired resistance mechanisms against anticancer drugs are the major limitations in the clinical routine. Regarding resistance characteristics, the significantly lower impact of p53 status on the responsiveness to the novel analogs compared with that to oxaliplatin is noticeable. With regard to platinum drugs, mutations in this major tumor suppressor gene were repeatedly reported to cause resistance (Arango et al., 2004; Hayward et al., 2004). HCT-116 p53/ko cells in comparison with the parental cell line were also significantly resistant against oxaliplatin in our study but to a distinctly lower degree for the novel analogs KP1537 and KP1691. Of interest, comparable although minor effects were detected by deletion of the p53 downstream targets bax and p21 in the case of oxaliplatin, whereas no impact on KP1537 was detected. Thus, we found no differences in cell cycle arrest but enhanced apoptosis induction by KP1537 compared with results for the other two compounds. Furthermore and as expected, cross-resistance to oxaliplatin-resistant cell models with both the p53/wt and p53/ko background was demonstrated for the novel substances. Here, an impact of stereoisomerism already became obvious. Whereas KP1691 was distinctly less cross-resistant against the acquired oxaliplatin-resistant cell models, KP1537 was in that case comparable to the parental compound. These data, together with the higher degree of DNA platination of the novel substances compared with that of oxaliplatin and the differences in drug export/import between KP1537 and KP1691, emphasize an impact of the steric orientation and indicate the possibility of different mechanisms of activity or detoxification pathways.

With regard to the in vivo experiments, two observations about the novel oxaliplatin analogs are especially noteworthy: the reduced dependence on the immunogenic cell death and the distinctly lowered adverse effects. In a recent study, it was shown that CT-26 murine colon cancer xenografts respond to oxaliplatin only in immunocompetent and not in immunocompromised mice (Tesniere et al., 2010). In subsequent studies, the molecular mechanisms of an oxaliplatin-induced “immunogenic cell death” were elucidated (Tesniere et al., 2010; Zitvogel et al., 2010). In contrast to oxaliplatin, cisplatin fails to induce such an immunogenic cell death (Martins et al., 2011). Similar to oxaliplatin, KP1537 and KP1691 were able to strongly retard tumor growth in immunocompetent BALB/c mice. Furthermore, preliminary data indicate that the novel substances are, in contrast to cisplatin and in accordance with oxaliplatin, able to induce parameters for immunogenic cell death such as activation of eukaryotic initiation factor eiF2α (data not shown). However, surprisingly, the novel analogs were also active in the immunodeficient background. Why the introduction of one methyl group might cause these differences is enigmatic and will be addressed by future studies.

On the basis of the equal anti-solid tumor but enhanced antileukemic activity, we decided to consider the stereoisomer KP1537 as the lead compound to evaluate acute adverse effects in comparison with those of oxaliplatin. Besides hematologic toxicities, peripheral neuropathies that involve cold thermal hypersensitivity are the major adverse effects of oxaliplatin-treatment in patients with colon cancer (Argyriou et al., 2008). In a recent study, it was shown that in BALB/c mice oxaliplatin also induces mechanical allodynia and cold hyperalgesia, accompanied by decreased nerve conduction velocity, neuronal atrophy, and multinucleated dorsal root ganglia neurons (Renn et al., 2011). In our hands, BALB/c mice had a significantly greater body weight loss when treated with oxaliplatin than with KP1537. In addition, the level of locomotor activity was significantly reduced in oxaliplatin-treated but not in KP1537-treated mice. These data are in accordance with another study, in which a tendency toward reduced locomotor activity was described after oxaliplatin treatment (Ta et al., 2009). Moreover, significant cold hypersensitivity was detected in oxaliplatin-treated but not KP1537-treated mice. These reduced adverse effects correspond to the enhanced maximal tolerated dose with administration on 3 consecutive days, allowing application of higher doses of the novel analogs and, thus, opening a wider therapeutic window (Abramkin et al., 2010). The mechanism of oxaliplatin neurotoxicity is still not fully elucidated. However, impacts of oxaliplatin on voltagegated sodium channels (Adelsberger et al., 2000; Webster et al., 2005), potassium and hyperpolarization-activated channels in nociceptors (Descoeur et al., 2011), and cation channels, such as the transient receptor potential ankyrin 1 (Nassini et al., 2011) have been reported. Moreover, a central role of the oxalate ligand in the cold hyperalgesia has been suggested (Sakurai et al., 2009). The clear-cut reduction by introduction of one methyl group in the cyclohexane ring would, at first glance, argue against this fact. However, our first short-time in vivo platinum accumulation experiments demonstrated that platinum contents (and probably also oxalate levels) in the sciatic nerve reached significantly higher levels with oxaliplatin than with KP1537. In contrast, platinum accumulation levels did not significantly differ in any other organs. This result suggests either specific exclusion or enhanced export of KP1537 from the peripheral nerves.

The data obtained in this study suggest that stereoisomerism might have distinct and complex effects on drug uptake, distribution, and anticancer activity in vitro and in vivo. Earlier studies of the impact of the DACH ligand stereoisomerism on the antiproliferative properties of oxaliplatin isomers revealed that the *trans*-configured *R,R*-DACH enantiomers are the most active representatives, including the oxaliplatin analogs investigated here (Abramkin et al., 2010). Thus, only the *R,R*-enantiomers were analyzed in the present study. The data obtained with regard to KP1537 and KP1691 demonstrate that only the orientation of the introduced methyl group can have a severe impact on drug accumulation and anticancer activity in several cancer types. Platinum accumulation levels in vitro might, on the one hand, reflect the increasing lipophilicity of the different oxaliplatin analogs in the following order: oxaliplatin < KP1691 < KP1537 (Rappel et al., 2005; Buss et al., 2011). On the other hand, an enhanced affinity of KP1537 for export mechanisms in the cell model tested seems to exist. However, a completely different platinum accumulation pattern was detected in the tumor tissue in vivo with minor changes in KP1537 accumulation over time. These observations indicate that different molecular factors are involved in vitro and in vivo, such as the presence of transport systems and altered drug metabolism, leading to altered tumor targeting and drug (in)activation. In that respect, it is interesting to mention that for DACH platinum stereoisomers also, no straightforward association between cellular accumulation and cytotoxic activity or in vivo efficacy exists (Pendyala et al., 1995). For example, the *cis-R,S*-DACH stereoisomer accumulated to higher levels than the *trans-S,S*-DACH compound but was significantly less active. However the *R,R*-DACH derivative was accumulated to the highest degree and was also the most active platinum complex. Taken together, our data imply that caution is needed when one is aiming to predict in vivo anticancer activity both from in vitro cytotoxicity and/or platinum accumulation data.

In summary, we demonstrate that minor modifications on the cyclohexane ring of oxaliplatin might profoundly alter both accumulation and activity parameters, resulting in analogs with improved therapeutic characteristics and reduced adverse effects, which should be further developed for potential clinical use.

Supplementary Material

Refer to Web version on PubMed Central for supplementary material.

Acknowledgments

We are indebted to Vera Bachinger for the skillful handling of cell cultures, Christian Balcarek for competent technical assistance, Irene Herbacek for fluorescence-activated cell sorting analysis, and Elisabeth Gal for animal care.

This work was supported by the Fonds zur Förderung der wissenschaftlichen Forschung [Grant FWF L568], Forschungsförderungsgesellschaft, the Genome Austria (GENAU) program (PLACEBO-Platform Austria for Chemical Biology) of the Austrian Council for Research and Technology Development.

ABBREVIATIONS

DACH	cyclohexanediamine
KP1537	[(1*R*,2*R*,4*R*)-4-methyl-1,2-cyclohexanediamine]oxalatoplatinum(II)
KP1691	[(1*R*,2*R*,4*S*)-4-methyl-1,2-cyclohexanediamine]oxalatoplatinum(II)
MTT	3-(4,5-dimethylthiazol-2-yl)-2,5-diphenyltetrazolium bromide
PI	propidium iodide
ANOVA	analysis of variance
wt	wild-type
ko	knockout
oxR	oxaliplatin-resistant cells

References

Abramkin SA, Jungwirth U, Valiahdi SM, Dworak C, Habala L, Meelich K, Berger W, Jakupec MA, Hartinger CG, Nazarov AA, et al. 1*R*,2*R*,4*R*)-4-Methyl-1,2-cyclohexanediamine}oxalatoplatinum(II): a novel enantiomerically pure oxaliplatin derivative showing improved anticancer activity in vivo. J Med Chem. 2010; 53:7356–7364. [PubMed: 20886814]

Abu Lila AS, Doi Y, Nakamura K, Ishida T, Kiwada H. Sequential administration with oxaliplatin-containing PEG-coated cationic liposomes promotes a significant delivery of subsequent dose into murine solid tumor. J Control Release. 2010; 142:167–173. [PubMed: 19861140]

Adelsberger H, Quasthoff S, Grosskreutz J, Lepier A, Eckel F, Lersch C. The chemotherapeutic oxaliplatin alters voltage-gated Na^+ channel kinetics on rat sensory neurons. Eur J Pharmacol. 2000; 406:25–32. [PubMed: 11011028]

Ali BH. Amelioration of oxaliplatin neurotoxicity by drugs in humans and experimental animals: a minireview of recent literature. Basic Clin Pharmacol Toxicol. 2010; 106:272–279. [PubMed: 20050845]

Arango D, Wilson AJ, Shi Q, Corner GA, Arañes MJ, Nicholas C, Lesser M, Mariadason JM, Augenlicht LH. Molecular mechanisms of action and prediction of response to oxaliplatin in colorectal cancer cells. Br J Cancer. 2004; 91:1931–1946. [PubMed: 15545975]

Europe PMC Funders Author Manuscripts

Argyriou AA, Polychronopoulos P, Iconomou G, Chroni E, Kalofonos HP. A review on oxaliplatin-induced peripheral nerve damage. Cancer Treat Rev. 2008; 34:368–377. [PubMed: 18281158]

Berger W, Elbling L, Minai-Pour M, Vetterlein M, Pirker R, Kokoschka EM, Micksche M. Intrinsic MDR-1 gene and P-glycoprotein expression in human melanoma cell lines. Int J Cancer. 1994; 59:717–723. [PubMed: 7960246]

Burger H, Zoumaro-Djayoon A, Boersma AW, Helleman J, Berns EM, Mathijssen RH, Loos WJ, Wiemer EA. Differential transport of platinum compounds by the human organic cation transporter hOCT2 (hSLC22A2). Br J Pharmacol. 2010; 159:898–908. [PubMed: 20067471]

Buss I, Garmann D, Galanski M, Weber G, Kalayda GV, Keppler BK, Jaehde U. Enhancing lipophilicity as a strategy to overcome resistance against platinum complexes? J Inorg Biochem. 2011; 105:709–717. [PubMed: 21450275]

Chaney SG, Campbell SL, Bassett E, Wu Y. Recognition and processing of cisplatin- and oxaliplatin-DNA adducts. Crit Rev Oncol Hematol. 2005; 53:3–11. [PubMed: 15607931]

Descoeur J, Pereira V, Pizzoccaro A, Francois A, Ling B, Maffre V, Couette B, Busserolles J, Courteix C, Noel J, et al. Oxaliplatin-induced cold hypersensitivity is due to remodelling of ion channel expression in nociceptors. EMBO Mol Med. 2011; 3:266–278. [PubMed: 21438154]

Fischer H, Taylor N, Allerstorfer S, Grusch M, Sonvilla G, Holzmann K, Setinek U, Elbling L, Cantonati H, Grasl-Kraupp B, et al. Fibroblast growth factor receptor-mediated signals contribute to the malignant phenotype of non-small cell lung cancer cells: therapeutic implications and synergism with epidermal growth factor receptor inhibition. Mol Cancer Ther. 2008; 7:3408–3419. [PubMed: 18852144]

Galanski M, Yasemi A, Slaby S, Jakupec MA, Arion VB, Rausch M, Nazarov AA, Keppler BK. Synthesis, crystal structure and cytotoxicity of new oxaliplatin analogues indicating that improvement of anticancer activity is still possible. Eur J Med Chem. 2004; 39:707–714. [PubMed: 15276304]

Goldberg RM, Sargent DJ, Morton RF, Fuchs CS, Ramanathan RK, Williamson SK, Findlay BP, Pitot HC, Alberts SR. A randomized controlled trial of fluorouracil plus leucovorin, irinotecan, and oxaliplatin combinations in patients with previously untreated metastatic colorectal cancer. J Clin Oncol. 2004; 22:23–30. [PubMed: 14665611]

Habala L, Galanski M, Yasemi A, Nazarov AA, von Keyserlingk NG, Keppler BK. Synthesis and structure-activity relationships of mono- and dialkyl-substituted oxaliplatin derivatives. Eur J Med Chem. 2005; 40:1149–1155. [PubMed: 16040163]

Hayward RL, Macpherson JS, Cummings J, Monia BP, Smyth JF, Jodrell DI. Enhanced oxaliplatin-induced apoptosis following antisense Bcl-xl down-regulation is p53 and Bax dependent: genetic evidence for specificity of the antisense effect. Mol Cancer Ther. 2004; 3:169–178. [PubMed: 14985457]

Heffeter P, Böck K, Atil B, Reza Hoda MA, Körner W, Bartel C, Jungwirth U, Keppler BK, Micksche M, Berger W, et al. Intracellular protein binding patterns of the anticancer ruthenium drugs KP1019 and KP1339. J Biol Inorg Chem. 2010; 15:737–748. [PubMed: 20221888]

Heffeter P, Jakupec MA, Körner W, Chiba P, Pirker C, Dornetshuber R, Elbling L, Sutterlüty H, Micksche M, Keppler BK, et al. Multidrug-resistant cancer cells are preferential targets of the new antineoplastic lanthanum compound KP772 (FFC24). Biochem Pharmacol. 2007; 73:1873–1886. [PubMed: 17445775]

Heffeter P, Jungwirth U, Jakupec M, Hartinger C, Galanski M, Elbling L, Micksche M, Keppler B, Berger W. Resistance against novel anticancer metal compounds: differences and similarities. Drug Resist Updat. 2008; 11:1–16. [PubMed: 18394950]

Jong NN, Nakanishi T, Liu JJ, Tamai I, McKeage MJ. Oxaliplatin transport mediated by organic cation/carnitine transporters OCTN1 and OCTN2 in overexpressing human embryonic kidney 293 cells and rat dorsal root ganglion neurons. J Pharmacol Exp Ther. 2011; 338:537–547. [PubMed: 21606177]

Jungwirth U, Kowol CR, Keppler BK, Hartinger CG, Berger W, Heffeter P. Anticancer activity of metal complexes: involvement of redox processes. Antioxid Redox Signal. 2011; 15:1085–1127. [PubMed: 21275772]

Kelland L. The resurgence of platinum-based cancer chemotherapy. Nat Rev Cancer. 2007; 7:573–584. [PubMed: 17625587]

Luo FR, Wyrick SD, Chaney SG. Biotransformations of oxaliplatin in rat blood in vitro. J Biochem Mol Toxicol. 1999; 13:159–169. [PubMed: 10098901]

Martins I, Kepp O, Schlemmer F, Adjemian S, Tailler M, Shen S, Michaud M, Menger L, Gdoura A, Tajeddine N, et al. Restoration of the immunogenicity of cisplatin-induced cancer cell death by endoplasmic reticulum stress. Oncogene. 2011; 30:1147–1158. [PubMed: 21151176]

McWhinney SR, Goldberg RM, McLeod HL. Platinum neurotoxicity pharmacogenetics. Mol Cancer Ther. 2009; 8:10–16. [PubMed: 19139108]

Nassini R, Gees M, Harrison S, De Siena G, Materazzi S, Moretto N, Failli P, Preti D, Marchetti N, Cavazzini A, et al. Oxaliplatin elicits mechanical and cold allodynia in rodents via TRPA1 receptor stimulation. Pain. 2011; 152:1621–1631. [PubMed: 21481532]

Pendyala L, Kidani Y, Perez R, Wilkes J, Bernacki RJ, Creaven PJ. Cytotoxicity, cellular accumulation and DNA binding of oxaliplatin isomers. Cancer Lett. 1995; 97:177–184. [PubMed: 7497460]

Pizarro AM, Sadler PJ. Unusual DNA binding modes for metal anticancer complexes. Biochimie. 2009; 91:1198–1211. [PubMed: 19344743]

Rappel C, Galanski M, Yasemi A, Habala L, Keppler BK. Analysis of anticancer platinum(II)-complexes by microemulsion electrokinetic chromatography: separation of diastereomers and estimation of octanol-water partition coefficients. Electrophoresis. 2005; 26:878–884. [PubMed: 15714548]

Reithofer MR, Valiahdi SM, Jakupec MA, Arion VB, Egger A, Galanski M, Keppler BK. Novel di- and tetracarboxylatoplatinum(IV) complexes. Synthesis, characterization, cytotoxic activity, and DNA platination. J Med Chem. 2007; 50:6692–6699. [PubMed: 18031001]

Renn CL, Carozzi VA, Rhee P, Gallop D, Dorsey SG, Cavaletti G. Multimodal assessment of painful peripheral neuropathy induced by chronic oxaliplatin-based chemotherapy in mice. Mol Pain. 2011; 7:29. [PubMed: 21521528]

Rosenberg B, Vancamp L, Krigas T. Inhibition of cell division in *Esche-richia coli* by electrolysis products from a platinum electrode. Nature. 1965; 205:698–699. [PubMed: 14287410]

Rosenberg B, VanCamp L, Trosko JE, Mansour VH. Platinum compounds: a new class of potent antitumour agents. Nature. 1969; 222:385–386. [PubMed: 5782119]

Sakurai M, Egashira N, Kawashiri T, Yano T, Ikesue H, Oishi R. Oxaliplatin-induced neuropathy in the rat: involvement of oxalate in cold hyperalgesia but not mechanical allodynia. Pain. 2009; 147:165–174. [PubMed: 19782472]

Shah N, Dizon DS. New-generation platinum agents for solid tumors. Future Oncol. 2009; 5:33–42. [PubMed: 19243296]

Stordal B, Pavlakis N, Davey R. Oxaliplatin for the treatment of cisplatin-resistant cancer: a systematic review. Cancer Treat Rev. 2007; 33:347–357. [PubMed: 17383100]

Ta LE, Low PA, Windebank AJ. Mice with cisplatin and oxaliplatin-induced painful neuropathy develop distinct early responses to thermal stimuli. Mol Pain. 2009; 5:9. [PubMed: 19245717]

Tesniere A, Schlemmer F, Boige V, Kepp O, Martins I, Ghiringhelli F, Aymeric L, Michaud M, Apetoh L, Barault L, et al. Immunogenic death of colon cancer cells treated with oxaliplatin. Oncogene. 2010; 29:482–491. [PubMed: 19881547]

Wang D, Lippard SJ. Cellular processing of platinum anticancer drugs. Nat Rev Drug Discov. 2005; 4:307–320. [PubMed: 15789122]

Wang X. Fresh platinum complexes with promising antitumor activity. Anti-cancer Agents Med Chem. 2010; 10:396–411.

Webster RG, Brain KL, Wilson RH, Grem JL, Vincent A. Oxaliplatin induces hyperexcitability at motor and autonomic neuromuscular junctions through effects on voltage-gated sodium channels. Br J Pharmacol. 2005; 146:1027–1039. [PubMed: 16231011]

Woynarowski JM, Chapman WG, Napier C, Herzig MC, Juniewicz P. Sequence- and region-specificity of oxaliplatin adducts in naked and cellular DNA. Mol Pharmacol. 1998; 54:770–777. [PubMed: 9804612]

Zitvogel L, Kepp O, Senovilla L, Menger L, Chaput N, Kroemer G. Immunogenic tumor cell death for optimal anticancer therapy: the calreticulin exposure pathway. Clin Cancer Res. 2010; 16:3100–3104. [PubMed: 20421432]

Europe PMC Funders Author Manuscripts

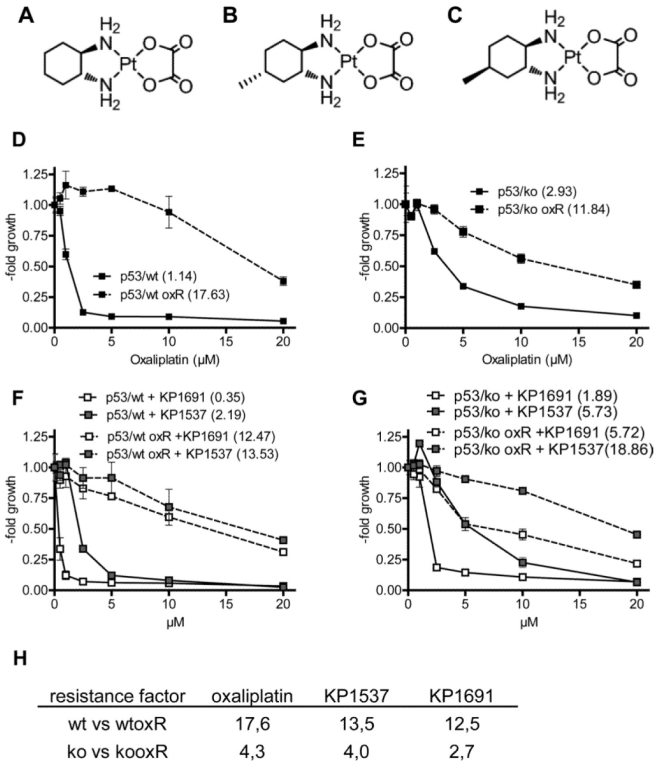

resistance factor	oxaliplatin	KP1537	KP1691
wt vs wtoxR	17,6	13,5	12,5
ko vs kooxR	4,3	4,0	2,7

Fig. 1.

Cross-resistance and impact of stereoisomerism. Chemical structures and stereochemistry of oxaliplatin (A), KP1537 (B), and KP1691 (C). Representative dose-response curves of oxaliplatin against HCT-116 p53/wt (D) and HCT-116 p53/ko (E) and their respective oxaliplatin-resistant cells (oxR). Comparison of cross-resistance of KP1537 and KP1691 against HCT-116 p53/wt and p53/wt oxR (F) and HCT-116 p53/ko and p53/ko oxR (G) cell models. IC_{50} values (micromolar) are given in parentheses. H, resistance factors calculated from IC_{50} values of dose-response curves.

Europe PMC Funders Author Manuscripts

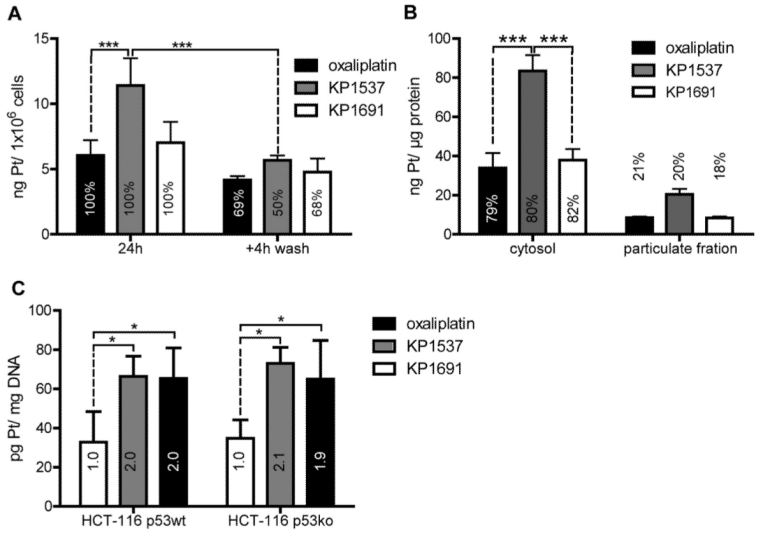

Fig. 2.

Platinum accumulation in vitro. A, platinum accumulation after 24 h of oxaliplatin, KP1537, or KP1691 treatment (10 μM) in HCT-116 p53/wt cells and after a washout phase (4 h). Values are expressed in nanograms of platinum·per 10^{-6} cells ± S.D. Numbers in columns indicate percentages of residual platinum content after washout. B, platinum content in the cytosolic and nucleic fraction after treatment of HCT-116 p53/wt cells with oxaliplatin, KP1537, or KP1691 for 24 h. Values are expressed in (nanograms of platinum)/(micrograms of protein) ± S.D. Distribution of each drug between cytosolic and nucleic fractions is given as a percentage. C, DNA platinum binding after 8 h of drug treatment in HCT-116 p53/wt and p53/ko cells. Fold differences in accumulation of oxaliplatin and novel compounds are indicated inside columns. Statistical analysis was performed by two-way ANOVA in A and Bonferroni post-test (*, $p < 0.05$; **, $p < 0.01$; ***, $p < 0.001$).

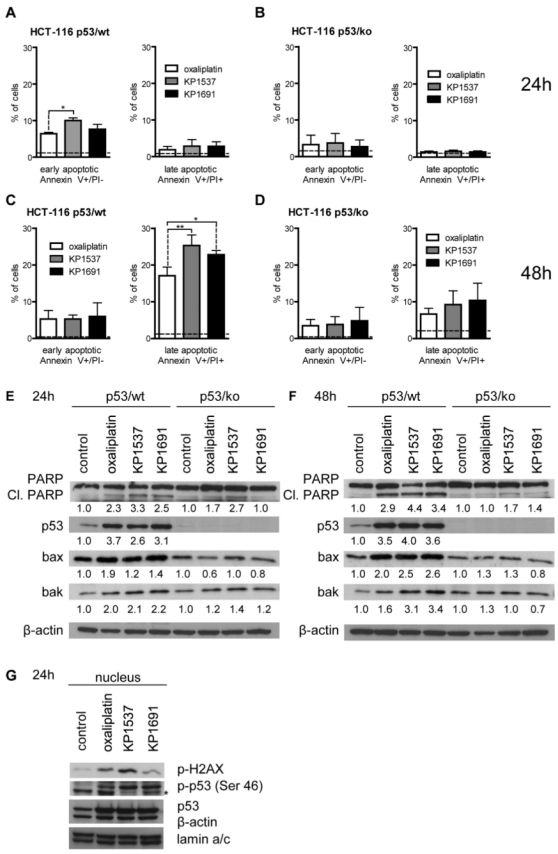

Fig. 3.

Induction of apoptosis in vitro. Induction of apoptosis was determined by annexin V staining of HCT-116 p53/wt (A and C) and p53/ko (B and D) cells after platinum drug treatment (10 μM) for 24 h (A and B) or 48 h (C and D). Mean percentages ± S.D. of early apoptotic (annexin V^+/PI^-) and late apoptotic cells (annexin V^+/PI^+) were determined from two independent experiments (*, $p < 0.05$; **, $p < 0.01$). Dashed lines indicate levels of early and late apoptotic cells in untreated control cells. Influences of novel oxaliplatin analogs on the expression of total and cleaved poly(ADP-ribose) polymerase (PARP), p53, and the indicated bcl-2 family members in HCT-116 p53/wt and p53/ko cells after 24 h (E) and 48 h (F) of treatment were determined by Western blotting. β-Actin served as the loading control. Numbers below lanes represent protein ratios relative to an arbitrary level of 1.0 assigned to the control sample. One of three experiments is shown. G, Western blot analysis of nuclear extracts determining phosphorylation of p53 (Ser46) and H2AX (Ser139). *, unspecific band. Lamin a/c served as the loading control.

Europe PMC Funders Author Manuscripts

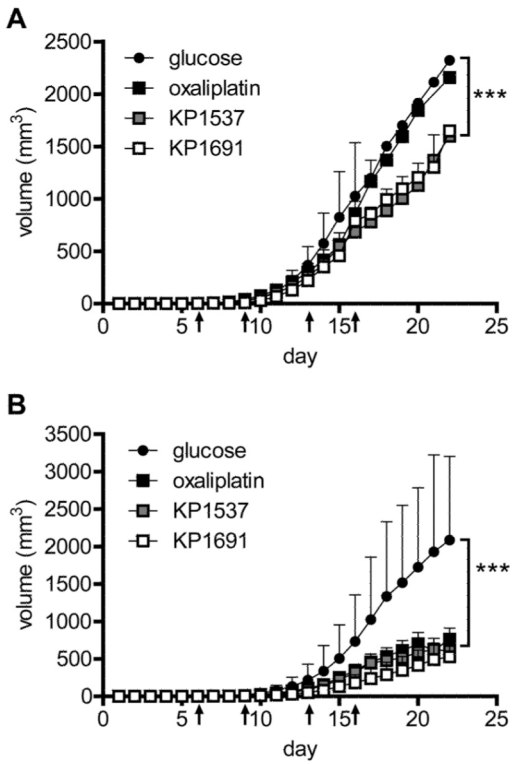

Fig. 4.

In vivo anticancer activity and accumulation. A and B, CT-26 cells (murine colon carcinoma) were injected subcutaneously in the right flank of SCID (A) and BALB/c mice (B). After the tumor was palpable, mice were treated for 2 weeks twice a week (days 6, 9, 13, and 16; arrows) with 9 mg/kg oxaliplatin, KP1537, and KP1691. Tumor volumes were calculated as described under *Materials and Methods*. Each experimental group contained five animals. Data are means ± S.D. Statistical analysis was performed by two-way ANOVA with Bonferroni post-test (*, $p < 0.05$; **, $p < 0.01$; ***, $p < 0.001$).

Europe PMC Funders Author Manuscripts

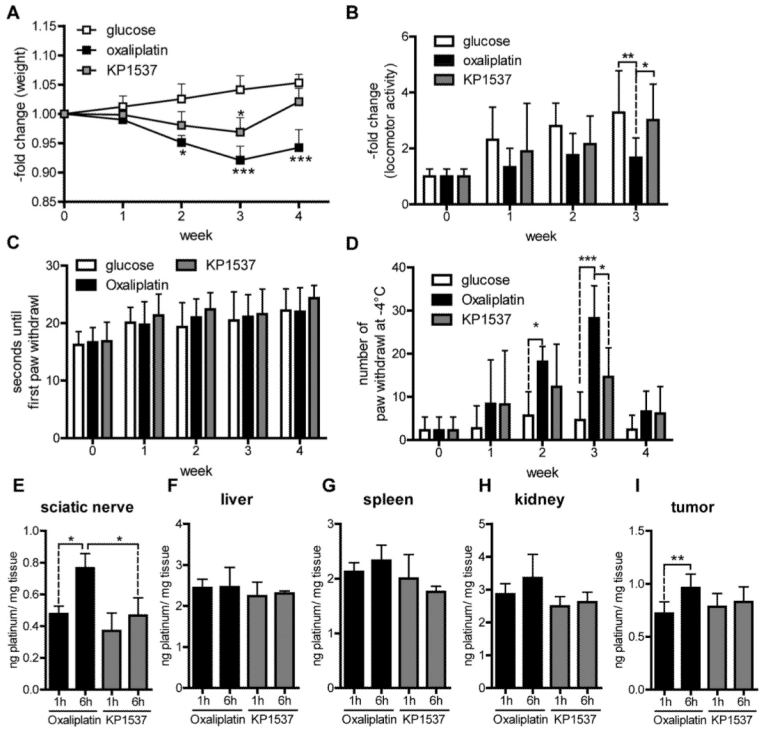

Fig. 5.

Adverse effects of KP1537 versus oxaliplatin. After baseline measurement (week 0), BALB/c mice were randomized to treatment groups ($n = 8$) of either 5% glucose solution (control), oxaliplatin (9 mg/kg), or KP1537 (9 mg/kg). Mice were treated intravenously for 2 weeks, twice per week. Changes in body weight (A), locomotor activity and explorative behavior (B), and nociceptive response latency in the hot-plate assay (+54°C) (C) before and after drug treatment are shown. Data are means ± S.E.M. D, number of paw withdrawals per minute on a (−4°C) cold plate. Platinum accumulation was measured in the sciatic nerve (E), liver (F), spleen (G), kidney (H), and tumor (I) after 1 and 6 h of oxaliplatin or KP1537 treatment. Values are expressed in terms of (nanograms of platinum)/(milligram of tissue) ± S.D. Statistical analysis was performed by two-way ANOVA and Bonferroni post-test (*, $p < 0.05$; **, $p < 0.01$; ***, $p < 0.001$).

Europe PMC Funders Author Manuscripts

Europe PMC Funders Author Manuscripts

TABLE 1

Anticancer activity of oxaliplatin, KP1537, and KP1691

IC_{50} values of diverse cell models and resistant sublines after 72 h, calculated from at least three independent dose-response curves.

Cell Line	Oxaliplatin		KP1537		KP1691	
	IC_{50}	RF	IC_{50}	RF	IC_{50}	RF
	μM		μM		μM	
MDA-MB-231	0.8 ± 0.3		1.2 ± 0.8		0.5 ± 0	
KB 3-1	1.5 ± 1.2		1.6 ± 1.1		0.6 ± 0.2	
A2780	0.4 ± 0.2		0.4 ± 0		0.3 ± 0.1	
K-562-S	1.3 ± 1		1.1 ± 0.1		0.6 ± 0.2	
HL-60	0.6 ± 0.2		0.7 ± 0.3		0.3 ± 0.1	
L1210[a]	0.6 ± 0.1		0.6 ± 0.4		0.6 ± 0.1	
RPMI-8226	0.5 ± 0.2		0.5 ± 0.3		0.4 ± 0.2	
GLC-4	0.8 ± 0.3		0.8 ± 0.1		0.3 ± 0.2	
A549	11.5 ± 3.9		7.5 ± 0.6		3.9 ± 2.3	
HCT-116 *p21*(+/+)	1.7 ± 0.4		2.8 ± 0.8		0.6 ± 0.1	
HCT-116 *p21*(−/−)	2.7 ± 0.2	1.5	3.2 ± 0.3	1.2	1 ± 0.1	1.7
HCT-116 *bax*(+/+)	0.9 ± 0		1.8 ± 0.5		0.6 ± 0.1	
HCT-116 *bax*(−/−)	1.4 ± 0.5	1.6	1.9 ± 0.9	1	0.7 ± 0.1	1.2
HCT-116 *p53*(+/+)	1.2 ± 0.5		2.3 ± 0.4		1 ± 0.5	
HCT-116 *p53*(−/−)	3.7 ± 1.2	3.1	5.3 ± 1.7	2.3	1.7 ± 1.2	1.7
SW480	0.9 ± 0.3		1.5 ± 0.1		1.2 ± 0.5	
CT-26[a]	2.4 ± 0.5		4.9 ± 0.3		2.1 ± 0.4	
Mean	1.9		2.2		1.0	

RF, resistance factor.

[a]Murine origin.